AIAA JOURNAL
Vol. 40, No. 6, June 2002

Stark Broadening and Stimulated Raman Pumping in High-Resolution N_2 Coherent Anti-Stokes Raman Scattering Spectra

M. A. Woodmansee*
General Electric Corporate Research and Development Center, Niskayuna, New York 12309
R. P. Lucht†
Texas A&M University, College Station, Texas 77843
and
J. C. Dutton‡
University of Illinois at Urbana–Champaign, Urbana, Illinois 61801

In previous studies, the high-resolution N_2 coherent anti-Stokes Raman scattering (CARS) technique has been used to acquire pressure, temperature, and density measurements in high-speed supersonic flows. In these low-density flows, a tradeoff exists between elevating the CARS signal strength with increasing pump- and Stokes-laser intensities and introducing Stark broadening and stimulated Raman pumping effects into the high-resolution N_2 CARS spectra. To explore these laser-induced perturbations, the CARS technique is used to acquire $v = 0 \rightarrow 1$ and $v = 1 \rightarrow 2$ CARS spectra over a range of pressures in an optically accessible gas cell. By controlling the intensity of the pump- and Stokes-laser beams, Stark broadening effects in the high-resolution ($\Delta\omega = 0.10\ \text{cm}^{-1}$) broadband CARS spectra are explored. For pump-laser intensities greater than 185 GW/cm^2, the least-squares fits of the experimental spectra with theoretical spectra provide pressures and temperatures that diverge from conditions measured within the cell using conventional transducers for pressures and temperatures around 0.2 atm and 298 K, respectively. An analytical model based on rigid-rotator harmonic-oscillator theory is used to describe how the increased optical fields of the pump and Stokes lasers stretch the molecular bond between the nitrogen nuclei, broadening and shifting the rotational transitions in the Q-branch manifold. Finally, by increasing the pump- and Stokes-laser intensities simultaneously, ambient $v = 1 \rightarrow 2$ N_2 CARS spectra, resulting from stimulated Raman pumping effects, are acquired with high resolution. Least-squares fits of these experimental spectra with theoretical spectra show that stimulated Raman pumping significantly increases the vibrational temperature extracted from the experimental spectra. The relative intensities of the rotational transitions in the $v = 0 \rightarrow 1$ manifold, however, are not affected by the stimulated Raman pumping process.

Nomenclature

A	=	cross-sectional area of laser beam at focus, m^2
B_e	=	rotational constant, cm^{-1}
c	=	speed of light in a vacuum, m/s
D_e	=	total dissociation energy, J
E	=	laser energy, J
$\bar{E}$	=	average electric field amplitude, V/m
F	=	force, N
$\hbar$	=	Planck's constant divided by 2π, J · s
I	=	laser irradiance or intensity, W/m^2; moment of inertia, kg · m^2
J	=	rotational quantum number
k	=	force constant, N/m
N	=	number density, molecules/m^3
p	=	pressure, atm
Q	=	vibrational transition with $\Delta J = 0$
q	=	internuclear separation, nm
r_w	=	$1/e^2$ beam radius, μm
T	=	temperature, K
t	=	time, s
u	=	Morse potential function
v	=	vibrational quantum number
z	=	Cartesian coordinate in plane normal to propagation of laser beam, m
α_e	=	vibration–rotation interaction constant, cm^{-1}
β	=	molecular Morse potential constant, cm^{-1}
Γ	=	transition linewidth, s^{-1}
Δ_j	=	population difference between rotational transitions
Δ_v	=	population difference between vibrational transitions
$\partial\alpha/\partial q$	=	polarizability derivative, m^2
$\partial\sigma/\partial\Omega$	=	Raman cross section, cm^2/sr
ε_0	=	permittivity of free space, C^2/J · m
μ	=	reduced mass, kg
ν	=	frequency, s^{-1}
ρ	=	spectral energy density, GW/(cm^2 GHZ)
χ_{CARS}	=	coherent anti-Stokes Raman scattering susceptibility
ω	=	circular frequency, rad/s or cm^{-1}
ω_e	=	vibrational wave number, cm^{-1}
$\omega_e\chi_e$	=	vibrational anharmonicity, cm^{-1}

Subscripts and Superscripts

e	=	equilibrium; electric field
J	=	rotational line
l	=	laser
max	=	maximum
p	=	pump laser

Presented as Paper 2001-0418 at the AIAA 39th Aerospace Sciences Meeting, Reno, NV, 8–11 January 2001; received 10 March 2001; revision received 9 November 2001; accepted for publication 21 November 2001.

*Mechanical Engineer, Combustion Laboratory, One Research Circle. Member AIAA.
†G. Paul Pepper Professor, Department of Mechanical Engineering. Associate Fellow AIAA.
‡W. Grafton and Lillian B. Wilkins Professor, Department of Mechanical and Industrial Engineering, 1206 West Green Street. Associate Fellow AIAA.

r = rotation; reaction
S = Stokes laser
t = total
trans = transducer
v = vibration
0 = initial or unperturbed state
$'$ = upper state
$''$ = lower state

Introduction

THE use of high-resolution N_2 coherent anti-Stokes Raman scattering (CARS) for both time-averaged and single-laser-shot measurements of pressure, temperature, and density in high-speed gas flows has been recently demonstrated.[1,2] This broadband CARS technique is a nonintrusive method that resolves the rotational transitions of the $v=0\rightarrow 1$ N_2 Q branch to within $\Delta\omega=0.10$ cm^{-1}, taking advantage of the line broadening and population shifts of these discrete rotational modes, which are pressure and temperature sensitive.

At low laser intensities, CARS is a nonperturbing process whereby the shape of the collected N_2 CARS spectrum is independent of the pump- and Stokes-laser intensities used to generate the CARS spectra. More specifically, CARS is a parametric process whereby the nonlinear interaction of the laser pulses with the probed molecule introduces no population changes within the rotational and vibrational manifolds of the molecules. When focused high-intensity pulsed-laser radiation is used, the intermolecular forces induced by the electric field of the laser may become comparable with the electronic binding forces between the nuclei of the irradiated molecules. Under these conditions, the CARS spectrum may be modified through a process known as Stark broadening (SB) (see Refs. 3–5). Also, for high-intensity resonant laser radiation, stimulated Raman pumping[6–13] (SRP) may become an important interference in the CARS measurements. In some instances, these laser-induced perturbations will alter the rotational and vibrational transition intensities of the N_2 CARS spectra, subsequently modifying the pressures and temperatures extracted from the data by least-squares fitting of theoretical spectra to the experimental spectra.

To examine the effects of SB and SRP, high-resolution broadband N_2 CARS is used here to collect $v=0\rightarrow 1$ and $v=1\rightarrow 2$ spectra at known pump- and Stokes-laser intensities in an optically accessible room-temperature gas cell. This broadband technique has a distinct advantage over previous studies employing narrowband pump and Stokes lasers in that the entire ro-vibrational manifold is excited for each laser pulse of the broadband system. Laser perturbation studies using narrowband pump and Stokes lasers may bias the collected CARS spectra by exciting only a very narrow region ($\Delta\omega_S\approx 0.1$ cm^{-1}) of the Q-branch envelope. Similarly, as already mentioned, the high-resolution CARS detection system employed here surpasses the resolution of other reported broadband CARS systems,[6] for example, $\Delta\omega=5$ cm^{-1}. This detection system captures the behavior and interaction of the dense cluster of rotational lines near the vibrational bandhead, which are pressure and temperature sensitive.

Experimental CARS spectra subject to varying degrees of SB are first presented. The effect of SB on the least-squares fits of the experimental spectra with theoretical spectra is quantified, illustrating the variation in deduced temperature and pressure with increasing pump-laser intensity. A SB model based on rigid-rotator harmonic-oscillator theory is then presented. This model provides qualitative insight into the line broadening and shifting of the rotational transitions in the vibrational manifold with increasing optical field strength. Finally, this paper concludes with a presentation of experimental $v=1\rightarrow 2$ CARS spectra generated by SRP processes. A spectral synthesis code, used for least-squares fitting of the experimental data, highlights the strong disagreement between the rotational temperature T_r and vibrational temperature T_v caused by $v=0$ to $v=1$ SRP.

Background

A tradeoff exists in most CARS experiments between maintaining an adequate signal-to-noise ratio (SNR) and preventing unwanted laser-induced perturbations in the CARS spectra. Unfortunately, during the course of CARS experiments, it is difficult to identify the laser-intensity thresholds at which the SB and SRP effects begin to appear in the collected CARS spectra.

In the CARS probe volume, it is possible for the strong optical fields imposed by the coherent pump and Stokes lasers to alter the spacing between the nitrogen nuclei. The term optical field is used here to describe both the coherent electric and magnetic fields associated with each laser pulse. However, as described by Maxwell's equations (see Ref. 4), it is the electric field, not the magnetic field, that displaces the atoms in a molecule with respect to their electron clouds. This displacement of the nuclei gives rise to an electric dipole, polarizing and reorienting the molecule in a direction that is related to the wave vector of the electric field. The applied electric field of each laser pulse stretches the chemical bond between the nuclei, shifting the discrete rotational and vibrational transitions of the molecule toward lower frequencies. This phenomenon is often called Stark shifting[3–5,14,15] in pure rotational CARS spectra and SB (see Refs. 3–5) in vibrational CARS spectra.

In this study, we probe a dense cluster of rotational lines [$Q(1)$–$Q(20)$] surrounding the ground vibrational manifold of the nitrogen molecule. The strong spatial and temporal variations in the electric fields of the two pump- and Stokes-laser pulses cause the rotational transitions near the $v=0\rightarrow 1$ bandhead to inhomogeneously broaden rather than shift. Hence, the CARS spectra collected here undergo SB rather than Stark-shifting processes. SB is a nonresonant phenomenon whereby the broadening and shifting of the rotational lines in the experimental CARS spectra are independent of the wavelength of the incident laser beam, that is, SB is an achromatic process. For example, to induce Stark shifts in H_2 rotational CARS spectra, Farrow and Rahn[14] and Rahn et al.[3] focused a separate 1.06-μm Nd:YAG beam onto the CARS probe volume. When spectra acquired with and without the presence of the infrared beam were compared, a 0.12-cm^{-1} shift toward lower frequencies was observed in the $S(3)$ transition of hydrogen when the external beam was present. This shifted rotational spectrum maintained an asymmetric line shape, most likely caused by the strong spatial and temporal gradients in the electric fields within the probe volume. Duncan et al.[7] found a similar, albeit smaller, Stark shift in the $v=1\rightarrow 2$ Q-branch spectrum of acetylene with increasing pump-laser intensities. Further experiments showed that the $v=1\rightarrow 2$ transition of acetylene is more susceptible to SRP than SB.

SRP, often called stimulated Raman scattering (SRS), is a two-photon scattering process whereby high pump- and Stokes-laser intensities drive the nitrogen molecules from the ground vibrational state to the first vibrational manifold, perturbing the vibrational population distribution. As shown in the energy-level diagram of Fig. 1, SRP couples the first two vibrational transitions of the CARS process in our experiments. When the pump- and Stokes-laser intensities are sufficiently high, SRP begins to perturb the vibrational population distribution by promoting molecules in the ground state to the first excited state, subsequently generating a vibrational hotband, or $v=1\rightarrow 2$ CARS spectrum. Ordinarily, when the temperature of the gas is less than 700 K, the hotband is weak and difficult to detect. However, with SRP, the $v=1\rightarrow 2$ Q-branch signal may be present regardless of the temperature of the gas. Clearly, this SRP-driven population redistribution will generate a difference between the vibrational temperature T_v and the rotational temperature T_r extracted from the CARS spectra (Ref. 16, p. 140).

Another deleterious effect of SRP stems from the saturation of the Raman rotational transitions in the $v=0\rightarrow 1$ Q-branch spectrum.

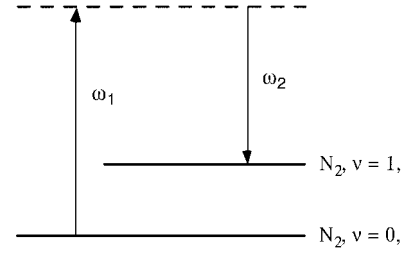

Fig. 1 Energy-level diagram of SRP process.

With higher pump- and Stokes-laser intensities, the number of molecules perturbed from the ground state to the first excited state increases until the Raman transitions begin to saturate (Fig. 1). Again, this promotion of molecules from the ground to the first vibrational level occurs before the CARS process is complete. This saturation decreases the molecular population difference, $N\Delta_v$, between the two vibrational energy levels, and this reduction in $N\Delta_v$ decreases the overall intensity of the CARS signal.

Duncan et al.[7] derived a theoretical model to predict the relative shift in the molecular population distribution between the ground and first vibrational levels of a probed molecule. Their analysis showed that the promotion of molecules in the ground state to the first vibrational transition is proportional to the product of the pump- and Stokes-laser intensities, that is, $I_p \cdot I_S$. Equally important, the amplitude of the CARS signal is a function of the product of all three input laser beams, $I_p^2 \cdot I_S$. Therefore, for certain combinations of pump- and Stokes-laser intensities, it is possible for SRP to compete with the CARS process. Using high pump- and Stokes-laser intensities, Gierulski et al.[6] collected $v = 0 \rightarrow 1$ through $v = 3 \rightarrow 4$ vibrational N_2 spectra using a broadband CARS system with a spectral resolution of $\Delta\omega = 5\ \text{cm}^{-1}$. Population redistributions on the order of 20% were found in the $v = 1 \rightarrow 2$ spectrum. However, the envelope formed by the rotational transitions in the ground vibrational state remained the same within experimental uncertainty over the range of pump- and Stokes-laser intensities studied. Although not quantified in the paper, based on the aforementioned observations, one would expect to find disagreement between the rotational and vibrational temperatures deduced from the spectra. Gierulski et al.[6] also found that SRP effects are more pronounced at reduced pressure, which is consistent with the experimental data to be presented.

Using an electrically heated oven, Kröll et al.[9] collected high-resolution $v = 0 \rightarrow 1$ and $v = 1 \rightarrow 2$ N_2 CARS spectra at 300 and 600 K. By employing a spectral synthesis code for least-squares fitting of the experimental spectra, the authors found that the best-fit rotational temperatures in both the $v = 0 \rightarrow 1$ and $v = 1 \rightarrow 2$ manifolds were within 5% of the oven temperature. However, for both operating conditions, the vibrational temperature exceeded 1400 K. The authors concluded that SRP had artificially populated the $v = 1 \rightarrow 2$ transition, raising the best-fit vibrational temperature. The rotational temperature, however, was unaffected by SRP because the saturation thresholds of the rotational transitions are approximately equal. Hence, the relative populations of the rotational transitions maintained a Boltzmann distribution (see Ref. 16) regardless of the perturbation of molecules in the ground vibrational state by SRP.

Equipment and Facilites

Figure 2 is a top-view schematic diagram of the high-resolution N_2 CARS system used in this study. The details of this system, for example, the type of Nd:YAG and broadband dye lasers (BDL), are found in Refs. 1 and 2. The primary feature of this optical arrangement is the CARS signal detection system, which comprises a 1.25-m spectrometer, relay lens pair, and an unintensified charge-coupled device (CCD) camera. These components enable this CARS system to acquire high-resolution ($\Delta\omega = 0.10\ \text{cm}^{-1}$) broadband N_2 CARS spectra on a single-shot basis. Typical CARS facilities used in combustion experiments have detection systems with limiting resolutions of $\Delta\omega = 0.5$–$1.0\ \text{cm}^{-1}$. The SPEX 1250M spectrometer has a 3200 line/mm holographic grating in a single pass Czerny–Turner configuration. At the exit of the spectrometer, a relay lens pair magnifies the image of the CARS spectrum by 7.5×. This relay lens consists of two Nikon camera lenses: an $f = 28$ mm and an $f = 210$ mm lens attached to the spectrometer exit and the CCD camera, respectively. The lenses are positioned so that their faces are nearly touching. The magnified CARS spectrum is captured by a Photometrics CH250 unintensified CCD camera with a 512×512 pixel array. The CARS spectra ensembles are collected and stored on an IBM-compatible personal computer.

For this study, half-wave plate and Glan polarizer assemblies are inserted in the path of the pump- and Stokes-laser beams to control the energy of each laser beam independently. For consistency with other such studies,[3,6,14] the pump- and Stokes-laser energies are reported here in terms of laser intensity or irradiance I. Laser energy E_i in joules, from source i, is converted into laser intensity I_i using the following relation:

$$I_i = E_i / A\Delta t_l \tag{1}$$

where A is the cross-sectional area of the laser beam at its focal waist and Δt_l is the time duration of a single laser pulse. Using a 500-MHz oscilloscope and a 1-ns-rise-time photodiode, the pulse duration of both the pump and broadband lasers was determined to be $\Delta t_l \approx 8$ ns full width at half maximum (FWHM). Estimates of the focal areas ($A = \pi r_w^2$) of the Nd:YAG and broadband laser beams were obtained by traversing a razor blade through the confocal region of each beam. The razor blade was mounted on a microtranslation stage to record blade position as a function of beam intensity. The Nd:YAG and BDL focal-spot radii, defined as $r = r_w$ at $1/e^2 \cdot I_{\max}$, were determined to be 13 and 23 μm, respectively, with an uncertainty of ± 1.5 μm. The beams were arranged in a folded BOXCARS[4] phase-matching configuration. Spherical lenses with a focal length of $f = 250$ mm were used to focus and then recollimate the CARS laser beams.

The high-pressure gas cell used in these experiments has optical access on all four sides, as shown in Fig. 2. The optical-port windows are constructed of 25.4-mm-thick, UV-grade fused silica; the faces of the windows are slightly biased (less than 5 arc-min) to prevent etaloning effects. For below atmospheric pressures, a vacuum pump is attached to the gas cell. A 1000-torr absolute pressure transducer (MKS 722A13TCE2FK) and a hermetically sealed thermistor (Omega ON-920-4007) are used to measure the cell pressure and temperature, respectively. The accuracy of the transducer is

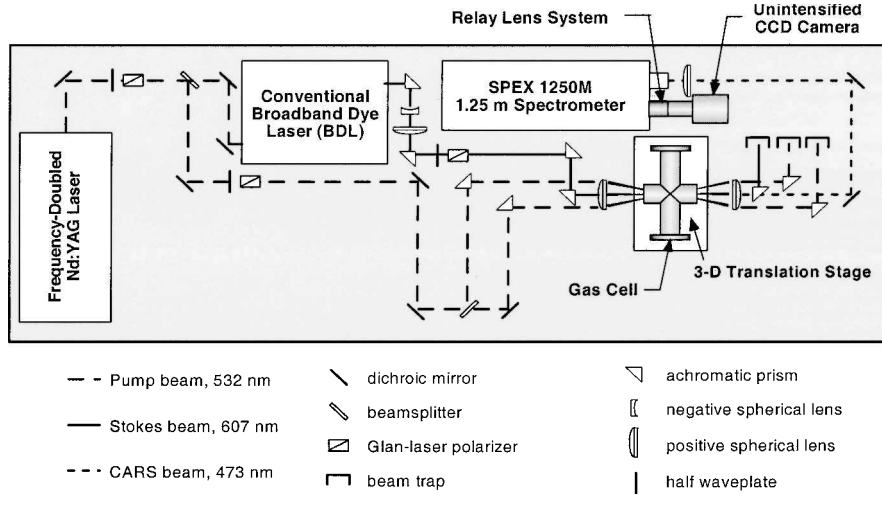

Fig. 2 Top-view schematic of high-resolution N_2 CARS system.

0.5% of reading; the accuracy of the thermistor is ±0.5°C. An MKS Type 660 readout and a Fluke 8050A digital multimeter monitor the pressure-transducer voltage and thermistor resistance, respectively. The nonlinear calibration curve for the thermistor was determined a priori using a constant-temperature bath and a ±0.2°C calibration thermometer.

Results and Discussion

Stark Broadening: Experiments

To isolate the effects of SB and SRP on the rotational structure of the $v=0\rightarrow 1$ and $v=1\rightarrow 2$ vibrational N_2 Q-branch transitions, time-averaged CARS spectra were acquired using various combinations of pump- and Stokes-laser intensities. Spectra were acquired at gas-cell pressures of $P=0.21$, 0.40, and 0.97 atm. SB and SRP effects are most evident in the CARS spectra acquired at subatmospheric pressures. Further, CARS spectra obtained at above atmospheric conditions, that is, high-molecular-number densities, proved to be not as susceptible to laser-induced perturbation effects. For brevity, only the 0.21- and 0.97-atm spectra ensembles are discussed here.

To highlight the differences between Stark-broadened and non-Stark broadened spectra, Fig. 3 shows two experimental CARS spectra collected at gas-cell conditions of $P=0.21$ atm and $T=293$ K. The Stokes laser intensity was held constant throughout the measurements. The spectra were acquired with pump-laser intensities of 329 GW/cm^2 (solid line) and 42 GW/cm^2 (dashed line). Because the CARS intensity is proportional to I_p^2, the spectrum acquired with the higher pump-laser intensity is normalized by the factor $42^2/329^2$ to allow direct comparison of the two spectra. The quantum-mechanical labels $Q(2)$ and $Q(4)$ are placed above their corresponding rotational lines at $\omega=2329.84$ cm^{-1} and $\omega=2329.57$ cm^{-1}, respectively, in Fig. 3. SB effects are most noticeable in these adjacent transitions. The intensity of the $Q(2)$ rotational transition is increased substantially at higher pump intensities. Interestingly, the susceptibility of the $Q(4)$ transition to SB effects is not as apparent. For the most part, the higher-J rotational transitions, that is, peaks to the left of the labeled transitions, in the Stark-broadened spectrum are less intense and broader than the transitions found in the low pump-laser intensity spectrum. Note that the broadening of the outer rotational lines is not homogeneous. As the peaks increase in linewidth, they become biased toward lower Raman shifts. More will be said about these trends when the SB model is presented in the next section.

Figure 4 shows least-squares fits of two experimental CARS spectra acquired in the gas cell at atmospheric conditions $P=0.97$ atm and $T=292$ K. The spectra in Figs. 4a and 4b are acquired with pump-laser intensities of $I_p=260$ GW/cm^2 and $I_p=51$ GW/cm^2, respectively. (I_p refers to the intensity of one of the two degenerate pump-laser pulses used in the folded BOXCARS phase-matching geometry.) Theoretical CARS spectra are shown as dashed lines in both plots. When the pump- and Stokes-laser linewidths, nonresonant susceptibility, gas pressure and temperature, and nitrogen mole fraction are specified, the spectral synthesis program CARSFIT[17] generates theoretical CARS spectra that are quantitatively compared to an experimental CARS spectrum. The CARSFIT program convolves the pump- and Stokes-laser linewidths with the nonlinear CARS susceptibility of the probed molecule. The program is automated so that the theoretical spectra may be least-squares fit to the experimental spectrum, using pressure and temperature as adjustable parameters in the fitting process. To evaluate or quantify the agreement between the experimental and theoretical spectra, CARSFIT employs a chi-square goodness-of-fit test.[18] CARSFIT, however, does not account for SB effects introduced by elevated laser intensities. Hence, by least-squares fitting experimental CARS spectra collected with increasing laser intensities with theoretical CARS spectra, the relative error induced by SB effects can be quantified.

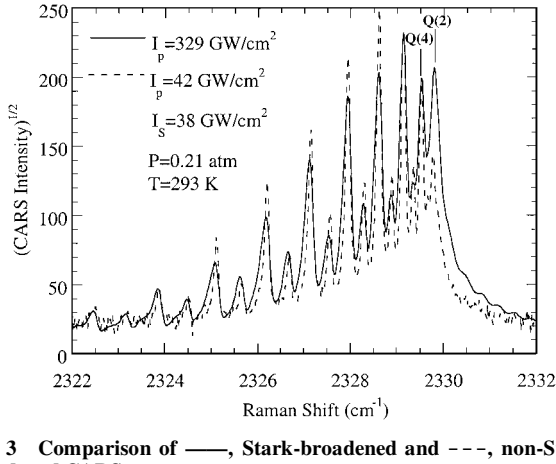

Fig. 3 Comparison of ——, Stark-broadened and – – –, non-Stark-broadened CARS spectra.

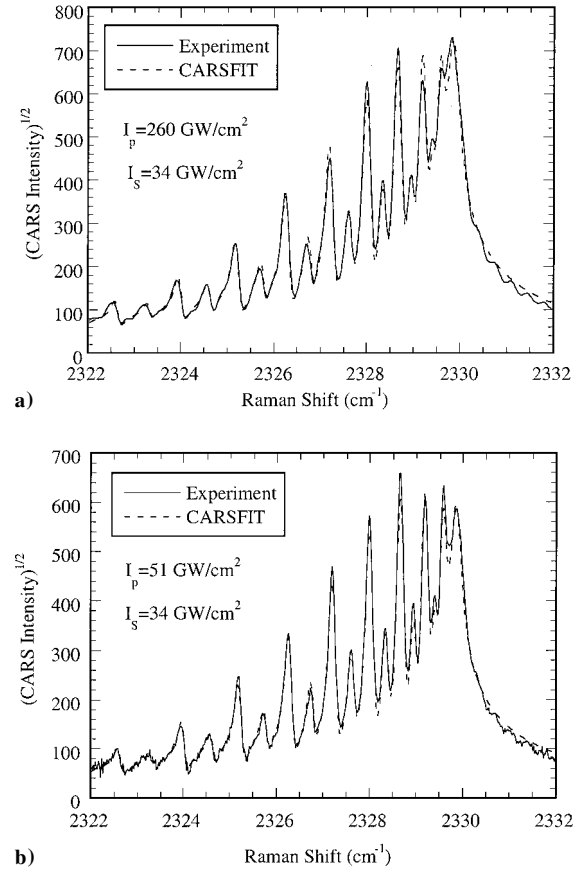

Fig. 4 Least-squares fits of a) Stark-broadened and b) non-Stark-broadened experimental CARS spectra.

SB effects similar to those found in Fig. 3 are evident in Fig. 4a. For instance, the intensity of the $Q(2)$ rotational transition is greater than the intensity of the $Q(4)$ transition. More important, the least-squares fit of the experimental spectrum in Fig. 4a yields pressure and temperature values of $P=1.20$ atm and $T=298$ K, respectively. Clearly, the intensity redistribution of the rotational transitions due to SB has increased the pressure extracted from the experimental CARS spectrum in Fig. 4a above that in the gas cell by approximately 24%. The best-fit CARS temperature is only slightly higher (2%) than the gas-cell temperature, indicating that SB primarily affects the pressure measurement. Unfortunately, the agreement between the experimental and theoretical spectra in Fig. 4a is quite good. One would hope that SB effects would alter the data to the point that CARSFIT could not match theoretical spectra to the experimental spectrum. However, Fig. 4a shows that SB modifies the experimental CARS spectra in such a way that the CARSFIT program is still able to fit the data but with the incorrect pressure. In a typical experiment for which the gas-cell pressure and temperature are not known a priori, it would be difficult to determine whether a CARS spectrum was subject to SB or simply reflects an altered gas-cell pressure.

Like Fig. 4a, the agreement between the experimental and theoretical CARS spectrum in Fig. 4b using lower pump-laser intensities is also quite good. The pressure and temperature extracted from the experimental spectrum, $P = 0.94$ atm and $T = 297$ K, respectively, are much closer to the actual conditions within the gas cell. However, as the noise in the wings of the CARS spectrum in Fig. 4b indicates, the lower pump-laser intensities used to generate this spectrum result in lower CARS signal strengths.

To determine a threshold pump-laser intensity below which SB effects are minimized, if not eliminated, experimental CARS spectra were collected as a function of increasing pump-laser intensity. These spectra were then fitted with theoretical spectra generated by CARSFIT. During the least-squares fit process, pressure and temperature were left as adjustable parameters. This study permits comparison of the best-fit pressure and temperature extracted from the experimental spectrum with the thermodynamic conditions in the cell, thereby quantifying the effect of SB on the optimal CARSFIT pressures and temperatures. In theory, the spectra generated at sub-atmospheric pressures ($P = 0.21$ atm) are more susceptible to SB effects due to the larger mean free path[19] between molecules. This physical explanation is confirmed later.

The influence of SB on the best-fit pressures and temperatures is shown in Figs. 5a and 5b, respectively. Uncertainty bars represent error in ΔT and ΔP due to 5% variation in minimum chi-square value provided by CARSFIT. The pressure difference ΔP between the transducer pressure and the pressure determined from the CARS spectrum, P_{CARS}, is shown along the ordinate of Fig. 5a, and the pump-laser intensity is plotted along the abscissa. During these measurements, the Stokes-laser intensity was held constant. Data ensembles collected at 0.21 and 0.97 atm are shown in Fig. 5. For the subatmospheric spectra collected with $I_p \leq 85$ GW/cm^2 in Fig. 5a, the disparity between the transducer and CARSFIT pressures stems from the low SNR of the CARS spectra. As shot noise and CCD read noise become comparable with the CARS signal level at lower pump-laser intensities, for example, $I_{\mathrm{CARS}} \sim I_p^2$, the ability of CARSFIT to mimic accurately the linewidth of the experimental spectrum diminishes. Note that, unlike narrowband CARS systems, the BDL energy is spread over a $\sim$130 cm^{-1} FWHM range centered about 607 nm. Hence, when a uniform energy density is assumed, only $\sim$8% of the energy from the BDL actually participates in the generation of the $v = 0 \rightarrow 1$ N_2 CARS signal. This inefficiency directly impacts the CARS signal strength.

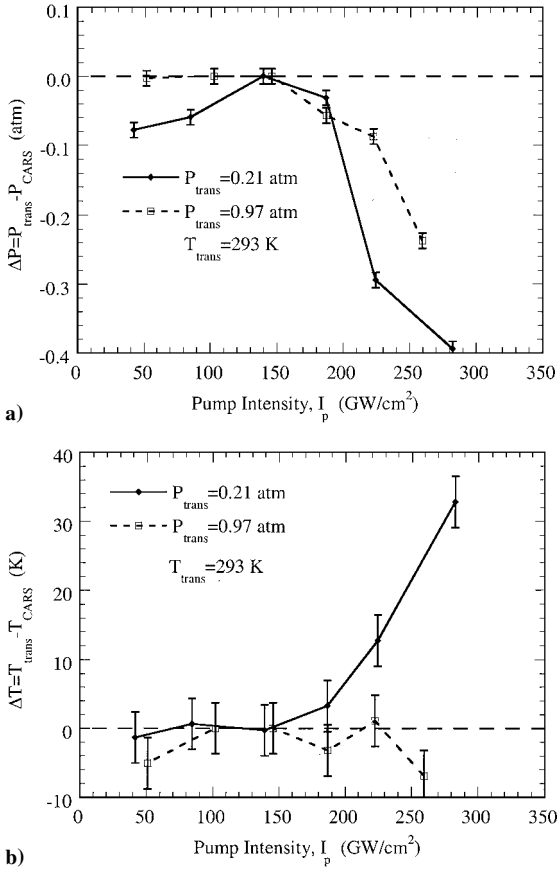

Fig. 5 Effects of pump-laser intensity on a) pressure and b) temperature extracted from time-averaged CARS spectra.

In Fig. 5a, ΔP rises toward zero with increasing pump-laser intensity and then decreases again, dropping off rapidly for $I_p > 185$ GW/cm^2. At these elevated pump-laser intensities, SB begins to noticeably modify the pressures extracted from the CARS spectra. Equally important, the optical breakdown of the gas prevents the acquisition of CARS spectra with pump-laser intensities greater than 280 GW/cm^2. Interestingly, for the atmospheric data ($P = 0.97$ atm), the effect of SB is not as predominant. Because the breadth of the rotational lines grows in proportion to the molecular number density, the line broadening due to the Stark effect becomes a smaller percentage of the overall rotational transition linewidth. Furthermore, the pressure difference ΔP does not decrease as rapidly as the downward trend in the 0.21-atm data ensemble. The optical breakdown threshold at 0.97 atm is lower (260 GW/cm^2) than at 0.21 atm.

In Fig. 5b, the subatmospheric temperature measurements show that the magnitude of $\Delta T = T_{\mathrm{trans}} - T_{\mathrm{CARS}}$ (where $T_{\mathrm{trans}} = 293$ K) increases in a nearly uniform manner for pump-laser intensities greater than 140 GW/cm^2. In fact, because of the pronounced effects of SB on the rotational line strengths of the N_2 CARS spectra collected at $P = 0.21$ atm, it proved to be very difficult to obtain good least-squares fits of the experimental spectra acquired above the SB threshold of $I_p > 185$ GW/cm^2. When this threshold is defined using the data presented in Fig. 5, only spectra acquired at pressures of 0.21 atm and above are absolved of SB effects. Interestingly, the CARS spectra collected at ambient conditions in Fig. 5b hover about $\Delta T = 0$ K. It is clear that at or above atmospheric conditions, SB plays a minimal role in modifying the best-fit pressures and temperatures. Supporting this statement, for spectra collected at 3 atm and above, optical breakdown of the gas preceded any noticeable effect of SB on the CARSFIT-deduced pressures and temperatures.

Based on the preceding results, pump-laser intensities of $I_p = 125$ GW/cm^2 were adhered to in other measurements[1,2] for which the thermodynamic conditions of the gas were unknown. Moreover, by operating at 67% of the pump-laser threshold of 185 GW/cm^2, it was possible to acquire spectra with $P < 0.21$ atm without inducing SB effects.

Stark Broadening: Model

To provide insight into the behavior of the experimental spectra described in the preceding section, a theoretical SB model is presented here. This model, based on rigid-rotator harmonic-oscillator theory, extends the work of Rahn et al.[3] to vibrational Q-branch transitions of homonuclear diatomic molecules. The goal of this model is to relate the intensity of the applied optical fields of the pump and Stokes lasers to the subsequent line broadening and population redistribution of the ro-vibrational transitions in the N_2 $v = 0 \rightarrow 1$ Q-branch spectra.

First, the center frequencies of a given rotational transition in a vibrational manifold is calculated by summing its rotational and vibrational components[4]:

$$\nu_J = \nu_v + \nu_r \tag{2}$$

By limiting this model to Q-branch transitions ($\Delta J = 0$), ν_r in Eq. (2) may be rewritten using molecule-specific harmonic and anharmonic rotational constants:

$$\nu_J = \nu_v + J(J+1)(B' - B'') \tag{3}$$

where $B' = B_e - \alpha_e(v' + \frac{1}{2})$ and $B'' = B_e - \alpha_e(v'' + \frac{1}{2})$. In Eq. (3), it is assumed that the vibration–rotation interaction constant α_e is not affected by the electrical fields of the pump and Stokes lasers. When only the $v = 0 \rightarrow 1$ Q-branch is considered, Eq. (3) simplifies to

$$\nu_J = \nu_v + \alpha_e J(J+1) \tag{4}$$

The preceding expression emphasizes that the applied optical fields alter the line strengths and linewidths of the ro-vibrational transitions via the vibrational frequency ν_v. This result is counterintuitive because one might expect that the changes in the moment of inertia of the molecule ($I = \mu q_e^2$) with increasing optical field strength would alter the line shape and relative population of the rotational transitions near the Q-branch bandhead. However, increasing the moment of inertia of the homonuclear molecules will induce SB or Stark shifting in only pure rotational transitions. Nevertheless, as will be shown, increasing the optical field strength of the pump and Stokes lasers will affect the vibrational frequency ν_v of the molecule in a uniform manner, altering the shape and relative population of the rotational modes in the Q-branch manifold.

According to classical mechanics, a molecule will absorb or emit radiation with a frequency of

$$\nu_v = (1/2\pi)(k/\mu)^{\frac{1}{2}} \tag{5}$$

when it changes its quantized vibrational state ($\Delta v = \pm 1$). In Eq. (5), k is the force constant, that is, spring constant, of the electronic bond between the two nitrogen atoms and μ is the reduced mass of the diatomic system. Taking the derivative of ν_v with respect to the internuclear spacing between the nitrogen nuclei, we find

$$\frac{\mathrm{d}\nu_v}{\mathrm{d}q} = \frac{1}{2}\frac{\nu_v}{k}\frac{\mathrm{d}k}{\mathrm{d}q} \tag{6}$$

Equation (6) shows that the shift in vibrational frequency is proportional to the change in force constant with respect to the internuclear spacing. As a first-order linear approximation, the preceding expression is expanded as

$$\frac{\delta\nu_v}{\nu_v} = \frac{1}{2k}\frac{\mathrm{d}k}{\mathrm{d}q}\delta q \tag{7}$$

where δq is defined as $\delta q \equiv q - q_0$ and q_0 is the spacing of the atoms at equilibrium in the ground electronic state. The variable ν_v is the unperturbed vibrational frequency, and $\delta\nu_v$ represents the finite shift in vibrational frequency with increasing internuclear spacing.

The Morse potential (see Ref. 20), often called the potential energy function, provides a method to determine the change in force constant with internuclear spacing, $\mathrm{d}k/\mathrm{d}q$. The Morse potential, given by

$$u(q - q_0) = D_e\left[1 - e^{-\beta(q-q_0)}\right]^2 \tag{8}$$

describes the motion of the nuclei in an electronic potential as a function of δq and the electronic binding energy D_e. As discussed by Herzberg,[21] the molecular constant β is defined as $\beta \equiv (2\pi^2 c\mu/D_e)^{1/2}\omega_e$. The force constant k is equivalent to[20]

$$k = \left(\frac{\mathrm{d}^2u}{\mathrm{d}q^2}\right)_{q=q_0} = 2D_e\beta^2 \tag{9}$$

Manipulating Eq. (9) further, the derivative of the force constant with respect to the internuclear separation of the atoms is

$$\frac{\mathrm{d}k}{\mathrm{d}q} = \left(\frac{\mathrm{d}^3u}{\mathrm{d}q^3}\right)_{q=q_0} = -6D_e\beta^3 \tag{10}$$

When it is assumed that the electronic bond between the atoms exhibits behavior similar to that of a classical spring, the change in internuclear spacing is related to the applied force of the electric fields via

$$\delta q = -F_r(z,t)/k \tag{11}$$

where the spring constant k is given in Eq. (9). The reactive force of the molecule, $F_r(z,t)$, is related to the amplitude of the electric field by the polarizability derivative[4] of the molecule,

$$F_r(z) = -\frac{\varepsilon_0}{2}\left(\frac{\partial\alpha}{\partial q}\right)_0\overline{E^2(z)} \tag{12}$$

The temporal dependence of the optical field has been removed from Eq. (12) by averaging over multiple light-wave periods. This averaging process is valid because the ground vibrational frequency of the nitrogen molecule is much less than the frequency of either the pump or Stokes optical wave trains, that is, $\omega_p, \omega_S \gg \omega_v$. In Eq. (12), the reactive force of a molecule becomes a function solely of z, the transverse spatial coordinate at the focus of the three signal-generating beams in the CARS probe volume.

The irradiance, or intensity, of the laser beams is related to the amplitude of their electrical fields by

$$I(z) = \tfrac{1}{2}c\varepsilon_0\overline{E^2(z)} \tag{13}$$

The preceding expression is derived from Maxwell's equations for plane electromagnetic waves. To maintain continuity with experimentally measured molecular constants, the differential Raman cross section[4] is substituted for the polarizability derivative using the following expression:

$$\frac{\partial\sigma}{\partial\Omega} = \frac{1}{64\pi^2}\frac{\hbar\omega_S^4}{\mu c^4\omega_v}\left(\frac{\partial\alpha}{\partial q}\right)_0^2 \tag{14}$$

Note that the Raman cross section is a strong function of the Stokes-laser frequency, which for the broadband laser of the current experiments is $\omega_S = 16{,}474\ \mathrm{cm}^{-1}$, that is, $\lambda_S = 607$ nm.

When Eqs. (9), (12), and (13) are inserted into Eq. (11), the following expression is obtained:

$$\delta q = \frac{4\pi}{D_e\beta^2}\sqrt{\frac{\mu c^2\omega_v}{\hbar\omega_S^4}}\left(\frac{\partial\sigma}{\partial\Omega}\right)^{\frac{1}{2}} I(z) \tag{15}$$

As shown, the increase in intermolecular spacing of the nuclei is linearly proportional to the intensity of the applied optical field. Finally, the change in vibrational frequency may be derived by substituting Eqs. (9), (10), and (15) into Eq. (7):

$$\frac{\delta\nu_v}{\nu_v} = -\frac{6\pi}{D_e\beta}\sqrt{\frac{\mu c^2\omega_v}{\hbar\omega_S^4}}\left(\frac{\partial\sigma}{\partial\Omega}\right)^{\frac{1}{2}} I(z) \tag{16}$$

The preceding expression is valid for the shift of a given rotational line J in the $v = 0 \rightarrow 1$ Q-branch envelope subject to an applied optical field, $I(z)$. With a nitrogen Raman cross section[22] of $\partial\sigma/\partial\Omega = 4.4 \times 10^{-31}$ cm^2/sr and a laser intensity of $I(z) = 300\ \mathrm{GW/cm^2}$, the shift in ro-vibrational line frequency given by Eq. (16) is $\delta\nu_v = -4.6$ GHz or $\delta\omega_v = -0.16\ \mathrm{cm}^{-1}$. This Stark shift is qualitatively consistent with the increase in linewidth of the rotational transitions in Fig. 3, although the calculated shift seems to be somewhat greater than the actual shift. Moreover, in Fig. 3, the Stark-broadened rotational lines are biased toward lower Raman shifts, which is consistent with the negative Stark shift calculated earlier.

In the CARS process, there are a total of three laser beams, two pump beams and one Stokes beam, which collectively alter the internuclear spacing between the nitrogen nuclei. To reflect this summation of electrical fields, Eq. (16) may be rewritten with the help of Eq. (4):

$$\nu_J = \nu_v\left[1 - \frac{6\pi}{D_e\beta}\sqrt{\frac{\mu c^2\omega_v}{\hbar\omega_S^4}}\left(\frac{\partial\sigma}{\partial\Omega}\right)^{\frac{1}{2}} I_T(z)\right] + \alpha_e J(J+1) \tag{17}$$

where $I_T = 2I_p + I_S$ is the spatially averaged aggregate intensity applied to the irradiated molecules by the pump- and Stokes-laser pulses. The expression to the right of the minus sign in the first parenthetical expression of Eq. (17) represents the decrease in vibrational frequency due to elevated pump- and Stokes-laser intensities. As already stated, the quantity ν_v is the unperturbed vibrational frequency of the molecule.

In Eq. (17), the shift of the rotational lines in the Q-branch manifold is directly related to the sum of the laser beam intensities.

As the optical field intensity is increased, the rotational lines will shift proportionately to lower frequencies. This result follows from the behavior of a classical harmonic oscillator in an electrical field. For Q-branch spectra, this shift manifests itself as a type of line broadening for two reasons. First, unlike pure rotational spectra, the rotational lines in the Q-branch manifold are not isolated transitions. Through the constructive interference terms in the CARS susceptibility χ_{CARS}, neighboring rotational lines have a pronounced effect on the line shape and line strength of other rotational transitions. Therefore, even though the Stark effect introduces a uniform shift [Eq. (17)] in the center frequency of all of the rotational lines in the Q-branch envelope, the line shape of the transitions does not maintain a self-similar profile with increasing optical field intensity due to the interaction of a given rotational mode with its neighboring transitions. This nonlinear interaction is accounted for when the CARS susceptibility is convolved with the pump- and Stokes-laser line shapes to synthesize theoretical CARS spectra.[4] To this end, one method to account for SB effects in the experimental Q-branch spectra is to incorporate Eq. (17) into the CARS susceptibility calculation in a spectral synthesis code such as CARSFIT, while adding the pump- and Stokes-laser intensities as user inputs. However, quantitative calculation of Stark-broadened spectra is complicated by the spatial and temporal profiles of the laser beams and the constructive and destructive interference fringes in the intensity pattern of the overlapping pump beams in the probe volume.

The second reason for the line shape and line strength alteration of the ro-vibrational transitions in Stark-broadened Q-branch spectra is the spatial variation of the laser intensity profiles within the CARS probe volume. For example, when it is assumed that the pump- and Stokes-laser beams maintain Gaussian amplitude distributions[4] with $r_w = 13$ and 23 μm focal diameters, respectively, the CARS signal intensity may be plotted as a function of the transverse distance at the intersection of the pump- and Stokes-laser beams. This profile is shown in Fig. 6. (Profiles have been normalized to enhance comparison.) Similarly, the SB amplitude distribution (ignoring interference fringes), $2I_p + I_S$, is plotted in Fig. 6 as well. (This result assumes that the beams are in a collinear phase-matching geometry, which approximates the BOXCARS phase-matching geometry used in this study.) Note that the two profiles in Fig. 6 have been normalized to facilitate comparison. In Fig. 6, the SB profile maintains the larger linewidth of 16-μm FWHM; the CARS signal linewidth is 10-μm FWHM. It is clear from Fig. 6 that the SB spatial profile varies in amplitude over the region where the CARS signal is generated. Based on this result, it can be inferred from Eq. (17) that the shift in rotational frequency varies across the probe volume or, more concisely, $\nu_J = f[\delta\nu_v(z)]$. This result implies that the collective spatial variation in the pump and Stokes lasers inhomogeneously broadens the rotational transitions rather than simply shifting the center frequency of the discrete rotational modes. The temporal profile of the laser pulses induces similar effects because the Stark shift will be a maximum at the peak of the laser pulse and minimal at the leading and trailing edges of the pulse.

Line-broadening effects are evident in the experimental CARS spectra of Fig. 3. As predicted, the rotational lines tend to broaden and decrease in strength at high pump-laser intensities ($I_p = 329$ GW/cm^2). The amplitude of the Stark-broadened rotational lines is on average 11% lower than the peaks of the rotational lines in the CARS spectrum not subject to high pump-laser intensities ($I_p = 42$ GW/cm^2). At the higher pump-laser intensity condition, the rotational-line broadening is biased toward lower frequencies, as predicted by Eq. (17). Furthermore, with the exception of the $Q(2)$ and $Q(4)$ lines near the bandhead, the increase in transition linewidth is nearly constant for all of the rotational modes in the Q-branch manifold. These observations support the arguments given earlier that the interaction terms in the CARS susceptibility and the optical field variations in the CARS probe volume filter the SB mechanism in such a way that the rotational transitions are broadened and shifted toward lower frequencies.

Stimulated Raman Pumping

When the Stokes-laser intensity is increased and the spectrometer is tuned to the $v = 1 \rightarrow 2$ N_2 CARS transition, stimulated Raman spectra were acquired in the optically accessible gas cell. Time-averaged spectra were acquired at 0.21 and 0.97 atm using a range of pump- and Stokes-laser intensities to generate the data. An experimental $v = 1 \rightarrow 2$ N_2 CARS spectrum, collected at 0.97 atm and 292 K, is shown in Fig. 7 (solid line). This hotband occurs over a lower Raman shift range, $\omega = 2292$–2302 cm^{-1}, than the $v = 0 \rightarrow 1$ transition. The $v = 1 \rightarrow 2$ CARS spectrum in Fig. 7 was generated using pump- and Stokes-laser intensities of 238 and 300 GW/cm^2, respectively. Because of low SNR of the $v = 1 \rightarrow 2$ CARS signal, the CCD chip was exposed for 1000 laser pulses. Similar to CARSFIT, a FORTRAN-based program called LineFit was used to perform least-squares fitting of the SRP spectra collected in this study (personal communication from R. L. Farrow, Sandia National Laboratories, Livermore, CA, 1998). The best-fit spectrum from this program is shown as a dashed line in Fig. 7. Whereas similar in many respects to CARSFIT, LineFit allows the rotational, T_r, and vibrational, T_v, temperatures to be selected as parameters that are optimized in the least-squares fitting process.

In Fig. 7, the agreement between the experimental and theoretical spectra is quite good because the rotational line strengths and linewidths compare favorably. The spectral synthesis code is able to fit the asymmetric line shape of the smaller odd-J rotational lines in the $v = 1 \rightarrow 2$ manifold, as well as the transition between the resonant and nonresonant portions of the CARS signal at the right-hand edge of Fig. 7. Small line strength discrepancies between the experimental and theoretical spectrum exist in the $Q(6)$, $Q(8)$, and $Q(10)$ lines. The theoretical spectrum was generated with a best-fit vibrational temperature of $T_v = 1100$ K. The elevated theoretical temperature was necessary to simulate the laser-induced population of the $v = 1 \rightarrow 2$ transition. Of course, this vibrational temperature does not reflect the physical temperature of the gas within the cell. The best-fit rotational temperature of the $v = 1 \rightarrow 2$ spectrum, on

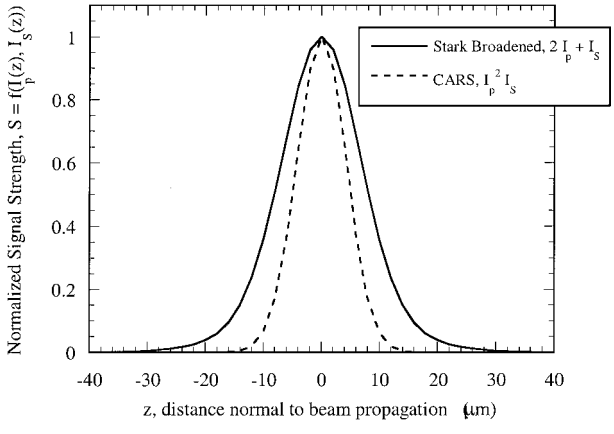

Fig. 6 Comparison of spatial variations of the SB amplitude profile ($2I_p + I_S$) with CARS signal strength ($I_p^2 I_S$) across CARS probe volume.

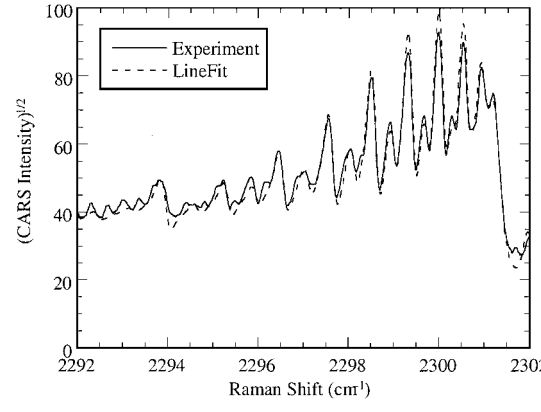

Fig. 7 Least-squares fit of $v = 1 \rightarrow 2$ N_2 CARS spectrum acquired at $P = 0.97$ atm and $T = 292$ K.

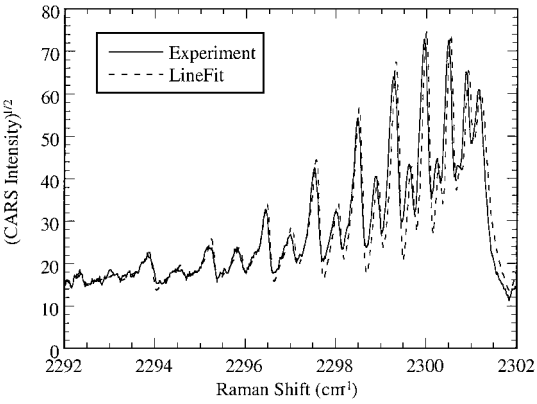

Fig. 8 Least-squares fit of $v = 1 \rightarrow 2$ N_2 CARS spectrum acquired at $P = 0.21$ atm and $T = 293$ K.

the other hand, is $T_r = 295$ K. This temperature, based on the relative population of the rotational lines in the $v = 1 \rightarrow 2$ band, is equal to the temperature of the air in the gas cell and 800 K less than the vibrational temperature. The agreement between the rotational temperature in the $v = 1 \rightarrow 2$ band and the gas-cell temperature indicates that the SRP rate from the lower $v = 0 \rightarrow 1$ vibrational manifold is approximately independent of J, as would be expected because of the small variation of the Raman cross section with J. Consequently, by increasing the Stokes-laser intensity, the rotational temperatures extracted from the $v = 0 \rightarrow 1$ CARS spectra do not deviate from the thermodynamic conditions of the air within the gas cell, so long as SB is negligible.

Figure 8 presents a $v = 1 \rightarrow 2$ CARS spectrum collected at 0.21 atm and 293 K. As is found with the $v = 0 \rightarrow 1$ spectrum collected at subatmospheric conditions, the rotational transitions in the $v = 1 \rightarrow 2$ manifold become more pronounced, that is, isolated, with decreasing pressure as collisional-broadening effects[23] diminish. Similar to Fig. 7, a theoretical spectrum (dashed line) is least-squares fit to the experimental spectrum (solid line). However, the agreement between the two spectra is not as good as the agreement found in Fig. 7. With the higher pump-laser intensities ($I_p = 288$ GW/cm^2) required to generate the spectrum in Fig. 8, it is possible that SB effects have altered the line shape and line strength of the rotational transitions in the $v = 1 \rightarrow 2$ spectrum. The Stokes-laser intensity is $I_S = 306$ GW/cm^2. The increased laser intensities are required to compensate for the decreased molecular number density in this experiment. The theoretical spectrum in Fig. 8 provides best-fit vibrational and rotational temperatures of $T_v = 1500$ K and $T_r = 295$ K, respectively. The increased discrepancy between the two temperatures ($\Delta T = 1200$ K) suggests that the efficiency of the Raman pumping process increases at subatmospheric pressures as would be expected because the collisional linewidths of the Q-branch lines are smaller.

The aforementioned discrepancy between the rotational and vibrational temperatures is consistent with the findings of Gierulski et al.[6] and Kröll et al.[9] Interestingly, Woodmansee et al.[2] found that the generation of a $v = 1 \rightarrow 2$ CARS spectrum does not affect the pressures and temperatures extracted from the $v = 0 \rightarrow 1$ CARS spectrum generated with the high-resolution N_2 CARS technique. Using pump- and Stokes-laser intensities of $I_p = 177$ GW/cm^2 and $I_S = 307$ GW/cm^2, single-shot $v = 0 \rightarrow 1$ CARS spectra were collected over a range of pressures (0.10–5.0 atm) in the optically accessible gas cell. At these pump- and Stokes-laser intensities, SRP does populate the $v = 1 \rightarrow 2$ CARS spectrum. The pressures extracted from the $v = 0 \rightarrow 1$ CARS spectra were on average 0.12 atm below the gas-cell pressure over the entire pressure range investigated, indicating excellent agreement between the CARS- and transducer-measured pressures. It is clear, however, from this study that the perturbation of the vibrational manifolds by SRP will directly affect the temperature recovered from vibrational CARS measurements at high temperatures.

One way to quantify the laser-intensity threshold at which SRP processes begin to populate the first vibrational transition is to compare the rate of molecular promotion, often called the slump rate,[24] with the duration of the laser pulse. The slump rate for monochromatic pump and Stokes lasers is given by[4,24]

$$\frac{1}{\Delta_v}\frac{\partial \Delta_v}{\partial t} = 2\left(\frac{4\pi c}{\hbar \omega_S^2}\right)^2 \left(\frac{\partial \sigma}{\partial \Omega}\right) \frac{\Gamma}{4(\Delta\omega_S)^2 + \Gamma^2} I_p I_S \qquad (18)$$

As expected, the rate of promotion from the ground vibrational state to the first vibrational state is proportional to $I_p \cdot I_S$. When it is assumed that a broadband Stokes laser embodies a uniform spectral energy density $\rho_S = I_S/\Delta\omega_S$ over the Raman line being probed, Eq. (18) may be integrated over the transition lineshape to obtain

$$\frac{1}{\Delta_v}\frac{\partial \Delta_v}{\partial t} = \pi\left(\frac{4\pi c}{\hbar \omega_S^2}\right)^2 \left(\frac{\partial \sigma}{\partial \Omega}\right) I_p \rho_S \qquad (19)$$

To prevent the population of the $v = 1 \rightarrow 2$ transition by SRP, the duration of the laser pulse must be much less than the rate at which the Raman pumping process is able to promote the molecules to a higher vibrational state. More succinctly,

$$\Delta t_l \ll \left(\frac{1}{\Delta_v}\frac{\partial \Delta_v}{\partial t}\right)^{-1} \qquad (20)$$

For example, when the pump- and Stokes laser intensities given in Fig. 7 and a broadband Stokes spectral width of $\Delta\omega = 1900$ GHz (100 cm^{-1}) are used, the right-hand side of Eq. (20) becomes

$$\left(\frac{1}{\Delta_v}\frac{\partial \Delta_v}{\partial t}\right)^{-1} = 0.4 \text{ ns}$$

This slump rate is one order of magnitude less than the laser pulse duration of $\Delta t_l = 8$ ns. Therefore, with this combination of high pump- and Stokes-laser intensities ($I_p \cdot I_S = 7.1 \times 10^4$ GW^2/cm^4), we should expect to generate a $v = 1 \rightarrow 2$ CARS spectrum. Equation (19) may also be used to calculate the minimum pump- and Stokes-laser intensity product that will not populate the $v = 1 \rightarrow 2$ CARS spectrum. For CARS spectra collected at ambient pressure in the gas cell, the product of the pump- and Stokes-laser intensities should not exceed $I_p \cdot I_S = 3.6 \times 10^3$ GW^2/cm^4 to prevent SRP. This result is qualitatively consistent with the observed presence of the $v = 1 \rightarrow 2$ CARS spectrum. For spectra collected at 2000 K, Eckbreth[4] suggests that the laser-intensity product not surpass $I_p \cdot I_S = 1$ GW^2/cm^4, which, when compared to the aforementioned threshold given by Eq. (19), is very low. Again, these lower laser intensities significantly decrease the CARS signal strength. The threshold given by Eckbreth[4] may apply only to narrowband CARS systems whereby the narrowband laser is tuned to a specific rotational transition in the CARS spectrum. As already stated, in broadband CARS, a large portion of the broadband laser's energy does not contribute to the generation of the CARS signal. Clearly, the product of the pump- and Stokes-laser irradiance is an important parameter for vibrational CARS measurements for which small changes in the laser intensities can significantly alter the population of the $v = 1 \rightarrow 2$ and higher[6] vibrational transitions.

Summary

In this study, $v = 0 \rightarrow 1$ and $v = 1 \rightarrow 2$ nitrogen Q-branch CARS spectra have been acquired in an optically accessible gas cell with a high-resolution N_2 CARS system. The experimental spectra, generated with known pump- and Stokes-laser intensities, were resolved to $\Delta\omega = 0.10$ cm^{-1} to study the effects of SB and SRP on the rotational line structure near the ground and first vibrational bandheads. The $v = 0 \rightarrow 1$ and $v = 1 \rightarrow 2$ spectra were least-squares fitted with theoretical spectra generated by spectral synthesis codes. The best-fit pressures and temperatures were then compared with the thermodynamic conditions measured by conventional transducers in the gas cell.

SB effects were induced in $v = 0 \rightarrow 1$ Q-branch spectra by increasing the pump-laser intensity above 185 GW/cm^2. As the pump-laser intensity is increased, the ro-vibrational lines broaden and decrease in strength. Also, a strong interplay between the $Q(2)$ and

$Q(4)$ lines near the bandhead was found at high pump-laser intensities. SB did not cause a distinct shift in the line structure. For laser intensities greater than 185 GW/cm^2, the pressures and temperatures extracted from the CARSFIT program diverged from the thermodynamic conditions within the cell. To help explain some of the characteristics of the Stark-broadened spectra, an analytical model of the SB mechanism, based on rigid-rotator harmonic-oscillator theory, was presented. Strong optical fields will increase the internuclear spacing between the nitrogen nuclei, decreasing the vibrational frequency component of the rotational lines in the Q-branch manifold. The decrease in vibrational frequency of individual rotational lines is complicated by their interaction with neighboring rotational lines via the cross-component terms in the CARS susceptibility. Similarly, the strength of the optical fields varies spatially within the CARS probe volume and temporally during the laser pulses, spreading the rotational transitions over a range of frequencies. These two conclusions support the inhomogeneous broadening of the rotational lines in the Stark-broadened $v = 0 \rightarrow 1$ CARS spectra presented here.

Through SRP, nitrogen $v = 1 \rightarrow 2$ CARS spectra were generated at room temperature in the gas cell by increasing the pump- and Stokes-laser intensities simultaneously. These experimental spectra were collected with the same resolution as the $v = 0 \rightarrow 1$ spectra. The best-fit vibrational temperature extracted from the ambient $v = 1 \rightarrow 2$ spectrum exceeded the temperature within the cell by 800 K. SRP, however, did not alter the linewidths or relative line strengths of the rotational transitions in the $v = 0 \rightarrow 1$ or $v = 1 \rightarrow 2$ CARS spectra. Accordingly, the best-fit rotational temperatures extracted from the experimental spectra were within 3 K of the temperature in the gas cell. Based on this observation, we conclude that the saturation thresholds for the different Q-branch rotational transitions in the CARS spectrum are approximately constant. A simple analysis shows that even incremental changes in the pump–Stokes intensity product $I_p \cdot I_S$ can generate SRP-populated $v = 1 \rightarrow 2$ spectra. This result is especially important for vibrational CARS studies in which the gas temperature is determined by comparing the molecular population of the $v = 0 \rightarrow 1$ and $v = 1 \rightarrow 2$ Q-branch manifolds.

Acknowledgments

Funding for this research was provided through the U.S. Army Research Office (Grant DAAG55-97-1-0194) with Thomas L. Doligalski as Contract Monitor. The authors are grateful for the assistance of Roger L. Farrow of Sandia National Laboratories in supplying the spectral synthesis codes used to least-squares fit the experimental spectra.

References

[1]Woodmansee, M. A., Dutton, J. C., and Lucht, R. P., "Experimental Measurements of Pressure, Temperature, and Density in an Underexpanded Sonic Jet Flowfield," AIAA Paper 99-3600, 1999.

[2]Woodmansee, M. A., Lucht, R. P., and Dutton, J. C., "Development of High-Resolution N_2 Coherent Anti-Stokes Raman Scattering for Measuring Pressure, Temperature, and Density in High-Speed Gas Flows," *Applied Optics*, Vol. 39, No. 33, 2000, pp. 6243–6256.

[3]Rahn, L. A., Farrow, R. L., Koszykowski, M. L., and Mattern, P. L., "Observation of an Optical Stark Effect on Vibrational and Rotational Transitions," *Physical Review Letters*, Vol. 45, No. 8, 1980, pp. 620–623.

[4]Eckbreth, A. C., *Laser Diagnostics for Combustion Temperature and Species*, Gordon and Breach, Amsterdam, 1996, Chaps. 1–4, 6.

[5]Péalat, M., Lefebvre, M., Taran, J.-P. E., and Kelley, P. L., "Sensitivity of Quantitative Vibrational Coherent Anti-Stokes Raman Spectroscopy to Saturation and Stark Shifts," *Physical Review A*, Vol. 38, No. 4, 1988, pp. 1948–1965.

[6]Gierulski, A., Noda, M., Yamamoto, T., Marowsky, G., and Slenczka, A., "Pump-Induced Population Changes in Broadband Coherent Anti-Stokes Raman Scattering," *Optics Letters*, Vol. 12, No. 8, 1987, pp. 608–610.

[7]Duncan, M. D., Oesterlin, P., König, F., and Byer, R. L., "Observation of Saturation Broadening of the Coherent Anti-Stokes Raman Spectrum (CARS) of Acetylene in a Pulsed Molecular Beam," *Chemical Physics Letters*, Vol. 80, No. 2, 1981, pp. 253–256.

[8]Farrow, R. L., and Lucht, R. P., "High-Resolution Measurements of Saturated Coherent Anti-Stokes Raman Spectroscopy Line Shapes," *Optics Letters*, Vol. 11, No. 6, 1986, pp. 374–376.

[9]Kröll, S., Aldén, M., Bengtsson, P.-E., and Löfström, C., "An Evaluation of Precision and Systematic Errors in Vibrational CARS Thermometry," *Applied Physics B*, Vol. 49, No. 6, 1989, pp. 445–453.

[10]Lucht, R. P., and Farrow, R. L., "Calculation of Saturation Line Shapes and Intensities in Coherent Anti-Stokes Raman Scattering Spectra of Nitrogen," *Journal of the Optical Society of America: B*, Vol. 5, No. 6, 1988, pp. 1243–1252.

[11]Shumay, I. L., Zadkov, V. N., Heinzen, D. J., Kash, M. M., and Feld, M. S., "Observation of the Saturation Effect in Continuous-Wave Coherent Anti-Stokes Raman Spectroscopy of Liquid Nitrogen," *Optics Letters*, Vol. 11, No. 4, 1986, pp. 233–235.

[12]Sparks, M., "Stimulated Raman and Brillouin Scattering: Parametric-Instability Explanation of Anomalies," *Physical Review Letters*, Vol. 32, No. 9, 1974, pp. 450–453.

[13]Zadkov, V. N., and Koroteev, N. I., "Saturation Effects in CARS: Collisionally Narrowed Raman Spectra of Diatomic Gases," *Chemical Physics Letters*, Vol. 105, No. 1, 1984, pp. 108–113.

[14]Farrow, R. L., and Rahn, L. A., "Optical Stark Splitting of Rotational Raman Transitions," *Physical Review Letters*, Vol. 48, No. 6, 1982, pp. 395–398.

[15]Péalat, M., and Lefebvre, M., "Temperature Measurement by Single-Shot Dual-Line CARS in Low-Pressure Flows," *Applied Physics B*, Vol. 53, No. 1, 1991, pp. 23–29.

[16]Incropera, F. P., *Introduction to Molecular Structure and Thermodynamics*, Wiley, New York, 1974, pp. 140, 198, 199.

[17]Palmer, R. E., "The CARSFT Computer Code for Calculating Coherent Anti-Stokes Raman Spectra: User and Programmer Information," Sandia National Labs., Rept. SAND89-8206, Livermore, CA, 1989.

[18]Hogg, R. V., and Tanis, E. A., *Probability and Statistical Inference*, Macmillan, New York, 1993, pp. 548, 554.

[19]Sonntag, R. E., and Van Wylen, G. J., *Introduction to Thermodynamics: Classical and Statistical*, Wiley, New York, 1991, p. 591.

[20]McQuarrie, D. A., *Statistical Thermodynamics*, Univ. Science, Mill Valley, CA, 1973, pp. 94, 110.

[21]Herzberg, G., *Spectra of Diatomic Molecules*, Van Nostrand Reinhold, New York, 1950, p. 101.

[22]Lapp, M., *Raman Short Course*, Sandia National Labs., Livermore, CA, 1980, Table 8.

[23]Siegman, A. E., *Lasers*, Univ. Science, Mill Valley, CA, 1986, pp. 126–130.

[24]Régnier, P. R., Moya, F., and Taran, J. P. E., "Gas Concentration Measurements by Coherent Raman Anti-Stokes Scattering," *AIAA Journal*, Vol. 12, No. 6, 1974, pp. 826–831.

W. R. Lempert
Guest Associate Editor